2011-05-01

All-fiber Polarimetric Electric Field Sensing Using Liquid Crystal Infiltrated Photonic Crystal Fiber.

Sunish Mathews
Dublin Institute of Technology, sunish.mathews@dit.ie

Gerald Farrell
Dublin Institute of Technology, gerald.farrell@dit.ie

Yuliya Semenova
Dublin Institute of Technology, yuliya.semenova@dit.ie

Recommended Citation

Mathews, S., Farrell, G., Semenova, Y. (2011) All-fiber Polarimetric Electric Field Sensing Using Liquid Crystal Infiltrated Photonic Crystal Fiber. *Sensors and Actuators A: Physical*, Volume 167, Issue 1, Pages 54-59, 2011. doi:10.1016/j.sna.2011.01.008

All-fiber polarimetric electric field sensing using liquid crystal infiltrated photonic crystal fibers

Sunish Mathews, Gerald Farrell, Yuliya Semenova
Photonics Research Centre, Dublin Institute of Technology, Dublin, Ireland
Email: sunish.mathews@dit.ie

Abstract

The operation of an all-fiber polarimetric electric field sensor based on nematic liquid crystal infiltrated photonic crystal fiber is demonstrated. A section less than 1 mm long of a selectively infiltrated polarization maintaining photonic crystal fiber is used as the probe. The transmission properties are studied for different lengths of the infiltrated section of the fiber subjected to an electric field. It is shown that the phase birefringence of the fiber can be controlled by adjusting the length of the infiltrated section subjected to an electric field, which allows for the sensor to have a linear transmittance response with the applied electric field intensity. The sensor is operated in the telecommunication window at 1550 nm and can be used for the fabrication of all-fiber electric field sensors for high and low electric field environments with an appropriate choice of liquid crystal material for infiltration and with optimization of the infiltration length.

Keywords:

All-fiber sensors; electric field sensing; liquid crystal infiltration; optical fiber sensor; photonic crystal fiber; polarimetric sensing scheme.

1. Introduction

Infiltration of photonic crystal fibers (PCF) with substances whose refractive index can be tuned by external electric fields allows for the dynamic modification of the guiding properties of the PCF. This property of infiltrated PCFs has been extensively studied for applications in various in-fiber tunable devices. Among the materials for infiltration, liquid crystals (LC) have received much attention due their external field dependent optical anisotropy and high birefringence. LC infiltrated solid core PCF has been utilised in various fiber tunable devices [1-4] and more recently for in-line tunable retarders and waveplates [5]. Infiltration of LC materials makes the PCF susceptible to external field variations, a property which can be utilized to fabricate all-fiber sensors for measurands such as temperature, magnetic field and electric field strength.

In this paper we present our evaluation of an all-fiber electric field sensor based on a nematic liquid crystal (NLC) infiltrated PCF. Fiber optic sensors for voltage and electric field measurement are widely used in the electric power industry. Unlike their conventional counterparts, fiber optic based electric field sensing techniques minimally disturb the electric field and are inherently immune to electromagnetic interference [6, 8]. They have several economic and performance advantages over conventional electronic sensors, most importantly they can provide true dielectric isolation in the presence of very high electric field strengths or voltages. A wide variety of fiber optic based electric field sensing schemes have been proposed and reported to date. These are mostly based on electro-optical crystals employed either in bulk optics or free-space type configurations or in an integrated waveguide type configuration [9-11]. However such schemes have a number of disadvantages such as high losses due to the presence of bulk optics, high coupling losses, costly integration with optical fiber, limited mechanical reliability and difficulties in large scale production. Small size, simple design and an all-fiber configuration with high measurement accuracy are major requirements for fiber based electric field sensors.

We report for the first time in this paper an electric field sensor that consists of a probe which utilises a section of a polarization maintaining photonic crystal fiber (PMPCF) selectively infiltrated with NLCs and which uses a polarimetric sensing scheme [12]. Since the birefringence of the infiltrated fiber is influenced by variations in the magnitude of an external electric field, the sensing mechanism is intrinsic to this type of sensor. The infiltration length is < 1mm and the lateral size of the sensor is ~ 125 microns which is the cladding diameter of the PCF, and therefore the sensing device is very compact, lightweight and can be easily attached to other optical fibers. A polarimetric sensing scheme is employed with the probe subjected to external electric fields applied perpendicularly to the PCF axis.

It is shown in this paper that varying the length of the infiltrated section influences the field induced phase retardance of the infiltrated PCF and thus allows for optimization of the electric field sensor characteristics such as sensitivity and the linear measurable electric field range. A study of the influence of the length of the infiltrated section subjected to the electric field and its effect on transmission loss in the PMPCF section is presented. The sensor operates in the telecommunication transmission window at an operating wavelength of 1550 nm.

2. Background

A cross-sectional view of the PMPCF used for our experiments is shown in figure 1. On infiltrating the two large holes of the PMPCF with the NLC mixtures the birefringent axis undergoes a 90° rotation [13]. The refractive index of the two holes is now set by the effective refractive index of the infiltrated NLC mixture. On the application of the electric field the LC molecules undergo reorientation and align themselves along the field direction, which changes the phase birefringence of the fiber. The overlap of the core mode of the PMPCF with the infiltrated LC in the two large holes allows for the fiber to exhibit a large variable birefringence on the application of an external electric field. Under these conditions the infiltrated PCF behaves as a variable phase retarder, with the retardance increasing with an increase in the length of the infiltrated section subjected to the applied electric field.

In a fashion similar to a Polarization Maintaining (PM) fiber, the PMPCF with its elliptical core supports two eigenmodes, with dominant electric field components in x and y directions (Figure 1). The eigenmodes are characterized by their effective refractive indices n_x and n_y. On infiltration and on the application of the electric field, the fiber birefringence changes to:

$$\Delta N = \left(n_{y0} - n_{x0}\right) - \left(n_{yE} - n_{xE}\right) \tag{1}$$

where n_{y0} and n_{x0} are the effective refractive indices in the absence of electric field and n_{yE} and n_{xE} are the effective indices with applied electric field. The phase retardance for the light propagating through the infiltrated PCF is given as,

$$\phi = \phi_0 + \phi_E \quad \text{, where} \quad \phi_E = \kappa_0 \Delta N L \tag{2}$$

Φ_0 is the inherent retardance of the infiltrated PCF and Φ_E is the phase retardance induced by the electric field, $\kappa_0 = 2\pi/\lambda$ is the wavenumber, λ is the free space wavelength and L is the length of the infiltrated section under the influence of an electric field.

Direct measurement of the effective indices of the modes of the infiltrated PMPCF is difficult and thus in order to characterize the retardance induced by the applied electric field it is convenient to express the field-induced phase retardance using the characterisation term E_π as follows:

$$\phi_E = \pi \frac{\Delta E}{E_\pi} \tag{3}$$

where ΔE is the change in electric field intensity. The sensor characterization term E_π can be measured by converting the phase shift into a change in the light intensity transmitted by the fibre using a linear polarizer. If the input and output polarizers are parallel and are at 45° with respect to the infiltrated PCF optical axis (n_y), the output intensity is given as,

$$I = \frac{I_0}{2}\left\{1 + \sin\left(\phi_0 + \pi \frac{\Delta E}{E_\pi}\right)\right\} \tag{4}$$

The transmitted intensity varies sinusoidally with electric field intensity and the period of oscillations is set by the electric field induced phase retardance term which depends on the length of the infiltrated section under the influence of the external electric field. The sensitivity of such a PMPCF fibre sensor to electric field increases with a decrease in the value of E_π. Since E_π is inversely proportional to the length of infiltration, the sensitivity of the device will increase as the length of the infiltrated section subjected to the applied electric field increases. In other words, a careful optimization of the infiltration length should allow for the design of sensors optimised for measurement in a specified electric field intensity range.

3. Sensor head and experimental setup

3.1. PCF and NLC mixtures used

The polarization maintaining PCF used for our experiments is the commercially available PM-1550-01 (Figure 1). It has five rings of air-holes around its asymmetric solid core. The small holes are of diameter ~ 2.2 μm and the two large holes defining the birefringent axis of the fibre have a diameter of 4.5 μm. The fiber has an asymmetric elliptical core, with a major axis 5.4 μm long and a minor axis 4.3 μm long. The intrinsic birefringence of the PM PCF is ~ 4.0 x 10^{-4} [14]. For our experiments the two large holes only are infiltrated with NLC mixtures. The nematic LC mixtures used for infiltration are MDA-05-2782 and MLC-7012 (Merck). The ordinary and extraordinary refractive indices of MDA-05-2782 are ~ 1.49 and ~ 1.61 respectively measured at 589.3 nm and the isotropic temperature of material is ~ 106 °C (Merck datasheet). The MLC-7012 material has an ordinary refractive index of ~ 1.464 and an extraordinary refractive index of ~ 1.53 measured at 589.3 nm (Merck datasheet). It has an isotropic temperature of 91 °C.

In order to examine the alignment of the Nematic LC mixtures in the PCF holes, each mixture was infiltrated into a silica capillary with ~ 5 micron inner diameter. Each capillary was then observed under a polarizing microscope. The alignment of MDA-05-2782 was found to be planar, whereas MLC-7012 was found to have a splayed alignment.

3.2 Fabricating the E-field sensor probe

A section (~ 30 mm) of the PMPCF is initially spliced to a Polarization Maintaining (PM) fiber pigtail using a standard fusion splicer. The fusion current, fusion time and number of arc discharges are optimized to achieve minimal air-hole collapse of the PMPCF at the splice joint and also to ensure minimal loss of the PM fiber structure at the splice joint [15]. The splice loss for the PMPCF to PM fiber joint is estimated to be ~ 6 dB.

The sensor head is a < 1 mm NLC infiltrated section of the PMPCF (Figure 1). Selective infiltration of the two large holes only is achieved by collapsing the smaller holes around the core using a standard fusion splicer. In order to achieve this, the cleaved end of the PMPCF is kept between the electrodes of the fusion splicer and controlled arc discharges are applied. The offset distance from the centre of the electrode axis, fusion current, fusion time are optimized in order to collapse all the smaller holes around the core leaving only the two large holes open [16].

The PCF is now infiltrated with nematic LC mixture by dipping the cleaved end of the PCF into a drop of the NLC mixture kept at room temperature. The infiltrated PCF is observed under a polarising microscope to ascertain the quality of infiltration and care was taken to ensure that both the holes of the PMPCF are evenly infiltrated. Uneven infiltration results in high insertion loss and sinusoidal spectral interference pattern formation. The collapsed end is cleaved off resulting in the total length of infiltration within the PCF after cleaving in the order of ~ 1 mm. This is done to minimise the insertion loss of the sensor, which increases with an increase in the length of infiltration. For MDA-05-2782 filled PMPCF an infiltration length of ~ 0.8 mm was observed using the polarizing microscope by cleaving after infiltration and for the MLC-7012 filled sample the infiltration length using the same method was ~ 1.6 mm. The disparity between the lengths achieved and the 1 mm desired length is a result of the limited accuracy with which the cleave length can be set. Furthermore due to the limitations of the translation stage on the polarizing microscope the measurement accuracy for the total infiltration length is ~ 0.1 mm. The infiltration of the LC mixture into the PCF introduces an insertion loss of ~ 6 dB at 1550 nm for both the NLC samples.

3.3 Experimental set-up

To test the feasibility of utilizing the selectively infiltrated PMPCF section for polarimetric electric field sensing the experimental set-up shown in figure 2 is employed. Light at 1550 nm from a tunable laser source is linearly polarised using a polarization controller (DPC5500; Thorlabs) and coupled into the input PM fiber with the selectively infiltrated PMPCF spliced to its other end. The PMPCF is clamped on to a precision bare fiber rotator and the rotator is mounted on a XYZ nano-positioner stage (1.0 micron translation accuracy). The infiltrated end of the PCF is kept between two electrodes with a spacing of ~ 150 microns between them. The fiber axis (n_y) of the PCF is arranged to be parallel with the electric field direction as in figure 1. This is done by using a fiber rotator and by viewing the end facet of the PMPCF under a high resolution digital microscope. The transmission of the infiltrated PCF in the presence of an external electric field is found to be dependent on the fiber optical axis orientation with respect to the direction of the electric field. With the axis of the fiber aligned along the electric field direction the electric field induced birefringence change is maximised.

The light transmitted by the PMPCF after passing through the infiltrated section is butt-coupled to an output PM fiber pigtail and is then coupled to the in-line polarimeter (IPM5300 Thorlabs). The butt coupling at the infiltrated end is done using another XYZ nano-positioner stage. The output from the polarimeter is passed through a free-space analyser and is then coupled to the optical detector to record the value of transmittance.

The electric field is applied to the infiltrated PCF using a combination of a high voltage power supply modulated by a standard waveform generator operating at 1 kHz. This provides a positive polarity voltage waveform that varies in time sinusoidally from zero volts up to a peak value, V_{peak}, with an average value of $V_{peak}/2$. The maximum value of V_{peak} used in the experiment is 1000 V. A common practice in measuring electric field intensity is to use the units of Volt-RMS per mm. Given the nature of the waveform used in our experiment the relationship between the V_{peak} value and the RMS value is given by: $V_{rms} = (3/8)^{1/2} V_{peak}$. In effect the sensing device is subjected to electric field intensity in the range from 0 to 4.1 kVrms/mm, given that the distance between the electrodes is ~ 150 microns.

In order to study the influence of the length of the infiltrated section under the electric field on the output transmittance, the infiltrated section is translated within the electrodes, using the input nano-positioner stage, in fixed length steps and the polarized transmittance is recorded in the range from 0 to 4.1 kVrms/mm. It should be mentioned that although a sinusoidally varying AC field is applied to the sensor head the polarized transmission data provided by the high-speed optical power meter is averaged over time. It is also possible to alter the infiltration length by

altering the quantity of LC material introduced into the PMPCF, but to achieve the equivalent fine increments in the infiltrated length for the purpose of this study would involve micro litre control of the infiltrated LC quantity which is difficult to achieve. It is for this reason that translation of the infiltrated section with respect to the electrodes is used as a more practical alternative.

4. Results and discussion:

4.1. MDA-05-2782 infiltrated PM-1550-01

Since the length of infiltration could not be estimated with accuracy better than 0.1mm, the initial adjustment for a length of the infiltrated section within the electrodes area was done by translating the PMPCF into the space between the electrodes up to the point when a noticeable change (~ 1 dB) in the output transmittance was observed between the zero and maximum values of the applied electric field. This length of the infiltrated section within the electrodes is taken as the reference point. The polarized transmission at 1550 nm for MDA-05-2782 infiltrated PM-1550-01 at different lengths of infiltrated section subjected to varying electric field is shown in figure 3. The infiltration length within the electrodes is incremented in 20 microns steps from the reference point and the electric field is varied from 0 to 4.1 kVrms/mm in each case. For the sample infiltrated with MDA-05-2782 the electric field threshold for LC molecular reorientation is estimated to be 2.0 kVrms/mm. Such a relatively large threshold is due to the planar alignment of this material within the holes of the PCF (the longer axes of the molecules coincides with the fibre axis z). Above the threshold field and with an increase in the length of the infiltrated section the phase retardance of the PMPCF increases.

As can be observed from the figure 3, the transmitted intensity above the threshold shows that the 60 microns infiltration length case provides the largest change in transmittance while also providing a monotonically decreasing response. Figure 4 shows the normalized transmittance response for the 60 microns sample along with a sinusoidal fit based on equation (4) for an electric field range from 2.0 kVrms/mm to 4.1 kVrms/mm. The value of E_π estimated from the fit is ~ 2.35 kVrms/mm. The built-in retardation term Φ_0 in equation (4) is a measure of the inherent phase retardance of the PMPCF and the phase retardance due to the infiltrated section outside the electrodes. It depends on various parameters such as temperature and stress on the PCF, and thus varies between measurements. In order to provide an estimate of the sensitivity of the device a linear response for an electric field can be assumed in the range from 3.4 - 4.1 kVrms/mm for the

60 micron sample. A linear fit for the data in this range provides an estimate of the sensitivity of the device as ~ 20 dB/kVrms/mm. Assuming an accuracy of 0.01 dB for the optical power measurement system, the estimated resolution of the device over this e-field intensity range is ~ 5 x 10^{-5} kVrms/mm (50 Vrms/m).

It should be noted that the PMPCF samples infiltrated with nematic LCs, have a planar alignment within the holes of the PCF and thus demonstrate threshold behaviour for the reorientation of the LC molecules. Therefore the field induced birefringence change can only be obtained above a threshold electric field [17]. The sensor's lower electric field measurement range in this case is limited by the threshold electric field.

4.2. MLC-7012 infiltrated PM-1550-01

Nematic LC mixtures with a splayed alignment do not show threshold effects [18]. Figure 5 shows the polarized transmittance at 1550 nm for MLC-7012 infiltrated PMPCF recorded for different lengths of the infiltrated section within the electrodes. The initial adjustment for the length of infiltrated section is carried out as explained in section 4.1. The infiltration length is incremented in steps of 50 microns from the reference point for this sample. Unlike the MDA-05-2782, the reorientation of LC molecules within the holes of the PCF takes place at very low values of the electric field. Since the birefringence of MLC-7012 is lower than that of MDA-05-2782, longer lengths of infiltrated section have to be subjected to the electric field to attain the phase retardance of the same order. A near linear response is obtained in the case with 150 micron length of the infiltrated section within the electrodes for the entire applied electric field range. Figure 6 shows the normalized transmission response obtained at this length of the infiltrated section within the electrodes. A fit based on equation (4) for an electric field range from 0 to 4.0 kVrms/mm is also shown. The value of E_π estimated from the fit is ~ 6.56 kVrms/mm. The MLC-7012 infiltrated PMPCF has a useful electric field measurement range from 0 to 4.0 kVrms/mm and by careful adjustment of the length of the infiltrated section within the electrodes the sensor can be fabricated so it has a linear electric field response using a measurement scheme based on transmission intensity. In this case a linear electric field range can be assumed for the 150 micron sample in range from 1.0 kVrms/mm to 4.1 kVrms/mm. On performing a linear fit the sensitivity in this case is estimated as ~ 2.0 dB per kVrms/mm. Assuming an accuracy of 0.01 dB for the optical power measurement system, the estimated resolution of the device over this e-field intensity range is ~ 5 x 10^{-3} kVrms/mm (~ 5 x 10^{3} Vrms/m).

The MDA-05-2782 infiltrated PMPCF sensor has a lower E_π value when compared to MLC-7012 infiltrated PMPCF sensor, and therefore displays a higher sensitivity to electric field intensity and thus a higher measurement accuracy than the MLC-7012 infiltrated PMPCF sensor. However the advantage of the MLC-7012 infiltrated PMPCF sensor is that it can operate from field intensities close to zero, whereas the MDA-05-2782 infiltrated PMPCF sensor only operates above a threshold electric field value.

With an appropriate choice of an LC mixture for infiltration and by controlling the length of infiltration these structures can be customized for measurement of electric field intensity in a specified electric field range. Given the high birefringence of the NLC mixtures available and the hole size of the PMPCF used, it is estimated that control on the infiltration length with an accuracy of ~ 1 μm is desirable, in order to achieve precise control of the electric field induced phase retardance. It should be mentioned that control on the length of infiltration (~ micron accuracy) is difficult to achieve with the standard procedure used by various authors for infiltrating PCFs (also used in our experiments). Acceptable control on the infiltration length within the PCF can be achieved by injecting a known quantity of LC mixture into the PCF using a controlled syringe pump arrangement with ~ 1μL volume delivery or by high precision fiber cleavers to obtain a required infiltration length by cleaving.

5. Conclusions

The performance of a nematic liquid crystal infiltrated polarization maintaining photonic crystal fiber as an all-fiber electric field sensor has been evaluated. The sensor probe is a < 1mm infiltrated section of the PMPCF and such a simple all-fiber design makes it very compact and allows for easy integration and coupling with fiber optics. A polarimetric scheme has been employed wherein the phase retardance of the selectively infiltrated PMPCF is controlled by carefully adjusting the length of the infiltrated section subjected to the electric field. By appropriate adjustment of the infiltration length within the electrodes the sensor can be optimized to provide a linear transmittance response to an external electric field. Nematic liquid crystal mixtures exhibiting both planar and splayed alignment within the holes of the PCF have been investigated. A sensor based on a splay aligned nematic LC mixture is shown to have a larger measurable electric field range, and consequently can be used for measurements of low electric field intensities. A planar aligned NLC mixture has improved sensitivity at high values of electric field. The nematic LC infiltrated PMPCF studied in this paper is capable of operating as an in-line

sensor for electric field intensity measurements using a source operating in the telecommunication window at 1550 nm. As an inherent electric field sensor the device can also be used as a voltage sensor with voltage being applied using a fixed electrode configuration. An appropriate choice of LC material for infiltration and the optimization of the infiltration length of selectively infiltrated PMPCFs would allow for the design and fabrication of compact, low loss, all-fiber electric field sensors for low and high electric field environments.

6. References

1. T. Larson, A. Bjarklev, D. Hermann, J. Broeng, Optical devices based on liquid crystal photonic bandgap fibres, Opt. Exp. 11 (2003) 2589-2596.
2. T.T. Alkeskjold, L. Scolari, D. Noordegraaf, J. Laegsgaard, J. Weirich, L. Wei, G. Tartarini, P. Bassi, S. Gauza, S.T. Wu, A. Bjarklev, Integrating liquid crystal based optical devices in photonic crystal fibers, Opt. Quant. Electron. 39 (2007) 1009-1019.
3. S. Ertman, T.R. Wolinski, D. Pysz, R. Buczynski, E.N. Kruszelnicki, R. Dabrowski, Low-loss propagation and continuosly tunable birefriengence in high-index photonic crystal fibers filled with nematic liquid crystals, Opt. Exp. 17 (2009) 19298-19310.
4. S. Mathews, Y. Semenova, G. Farrell, Electronic tunability of ferroelectric liquid crystal infiltrated photonic crystal fiber, Electron. Lett. 45 (2009) 617-618.
5. L. Wei, L. Eskildsen, J. Weiriech, L. Scolari, T.T. Alkeskjold, A. Bjarklev, Continuously tunable all-in-fiber devices based on thermal and electrical control of negative dielectric anisotropy liquid crystal photonic bandgap fibers, App. Opt. 48 (2009) 497-503.
6. V.M.N. Passaro, F. Dell'Olio, F. De Leonardis, Electromagnetic field photonic sensors, Prog. Quant. Elect. 30 (2006) 45-73.
7. C.G. Martinez, J.S. Aguilar, R.O. Valiente, An all-fiber and integrated optics electric field sensing scheme using matched optical delays and coherence modulation of light, Meas. Sci. Technol. 15 (2007) 3223-3229.
8. H. Togo, N. Kukutsu, N. Shimizu, T. Nagatsuma, Sensitivity-stabilized fiber-mounted electrooptic probe for electric field mapping, J. Lightwave. Technol. 26 (2008) 2700-2705.
9. M. Bernier, G. Gaborit, L. Du Villaret, A. Paupet, and J.L. Lasserre, "Electric field and temperature measurement using ultra wide bandwidth pigtailed electro-optic probes," App. Opt. 47, 2470-2476 (2008).

10. C. Li, and T. Yoshino, "Optical voltage sensor based on electrooptic crystal multiplier," J. Lightwave. Technol. 20, 843-849 (2002).
11. A. Michie, I. Bassett, J. Haywood, "Electric field and voltage sensing using thermally poled silica fibre with a simple low coherence interferometer," Meas. Sci. Technol. 17, 1229-1233 (2006).
12. T.R. Wolinski, "Polarimetric optical fibers and sensors," *Progress in Optics*, vol. XL, pp. 1-75, 2000.
13. S. Ertman, A. Czapla, K. Nowecka, P. Lesiak, A.W. Domanski, T.R. Wolinski, R. Dabrwoski, Tunable highly-birefringent photonic liquid crystal fibers, IEEE Instrumentation and measurement technology conference (2007) 1-6.
14. M. Szpulak, T. Martynkien, W. Urbanczyk, Effects of hydrostatic pressure on the phase and group modal birefringence in microstructured holey fibers, App. Opt. 43 (2004) 4739-4744.
15. L. Xiao, M.S. Demokan, W. Jin, Y. Wang, C. Zhao, Fusion splicing photonic crystal fibers and conventional single-mode fibers: microhole collapse effect, J. Lightwave. Technol. 25 (2007) 3563- 3574.
16. L. Xiao, W. Jin, M.S. Demokan, H.L. Ho, H.Y. Hoo, C. Zhao, Fabrication of selective injection microstructured optical fibers with a conventional fusion splicer, Opt. Exp 13 (2005) 9014-9022.
17. M.W. Haakestad, T.T. Alkeskjold, M.D. Nielsen, L. Scolari, J. Riishede, H.E. Engan, A. Bjarklev, Electrically Tunable Photonic Bandgap Guidance in a Liquid Crystal Filled Photonic Crystal Fiber, Photon. Tech. Lett. 17 (2005) 819-821.
18. L. Scolari, T.T. Alkeskjold, J. Riishede, A. Bjarklev, D.S. Hermann, A. Anawati, M.D. Nielsen, P. Bassi, Continuously tunable devices based on electrical control of dual frequency liquid-crystal filled photonic bandgap fibers, Opt. Exp. 13 (2005) 7483 – 7496.

Biographies:

Sunish Mathews graduated with BSc degree in Physics and MSc degree in Applied Physics from Mahatma Gandhi University, Kerala, India in 1999 and 2001 respectively. He worked as a research project assistant at Indian Institute of Technology Guwahati, Assam, India during the period 2005-2007. He joined the Photonics Research Centre of Dublin Institute of Technology (DIT) in Nov 2007 and is currently pursuing his PhD degree. His research interests include liquid crystal infiltrated photonic crystal fibers, in-fiber tunable devices and optical fiber sensors for electromagnetic field sensing, voltage and current sensing.

Gerald Farrell is the Head of School of the School of Electronic and Communications Engineering at the DIT. He graduated with an honours degree in electronic engineering from University College Dublin in 1979 and spent a number of years as a communications systems design engineer before joining the DIT. He received his PhD degree from Trinity College Dublin for research in all-optical synchronization using self-pulsating laser diodes. Prof. Farrell is also the Principal Investigator and Director of the Photonics Research Centre at the DIT. The centre's research concentrates on optical sensing, in particular FBG sensing, modelling and application of bend loss in optical fiber and photonic crystal fiber based sensors. He is the project leader on several research projects, some with international partners. Prof. Farrell has over 120 publications in the area of photonics, holds several patents and is a consultant for a number of well-known companies in the UK and Ireland.

Yuliya Semenova is a graduate of Lviv Polytechnic National University (Ukraine) of 1992. She received her PhD Degree in Physics of Liquid Crystals from the Ukrainian Academy of Sciences in 1999. Between 1997 and 2001 she worked as a researcher at the faculty of Electrophysics at the Lviv Polytechnic National University. Since 2001 she has been with the School of Electronic and Communications Engineering at Dublin Institute of Technology. She is a lecturer and senior researcher in the Photonics Research Center. Her research interests include liquid crystals, photonics and fiber optic sensing. She has published over 100 journal and conference papers.

List of figures and figure captions:

Figure 1. Selectively infiltrated PMPCF probe with axes orientation and applied field direction. Scanning electron microscope image of the PMPCF cross-section *(Bottom left; Fiber specification sheet; NKT Photonics).*

Figure 2. Schematic of the polarimetric e-field sensing set-up.

Figure 3. Transmission response of MDA-05-2782 filled PM-1550-01 at 1550 nm with varying electric field intensity obtained for different lengths of the infiltrated section between the electrodes.

Figure 4. Transmission response *(dots)* with 60 micron length of infiltrated section within the electrodes and its sine fit *(solid red line).*

Figure 5. Transmission response of MLC-7012 filled PM-1550-01 at 1550 nm with varying electric field intensity obtained for different lengths of infiltrated section under electrodes.

Figure 6. Transmission response *(dots)* with 150 micron length of infiltrated section within the electrodes and its sine fit *(solid red line).*

Figure 1:

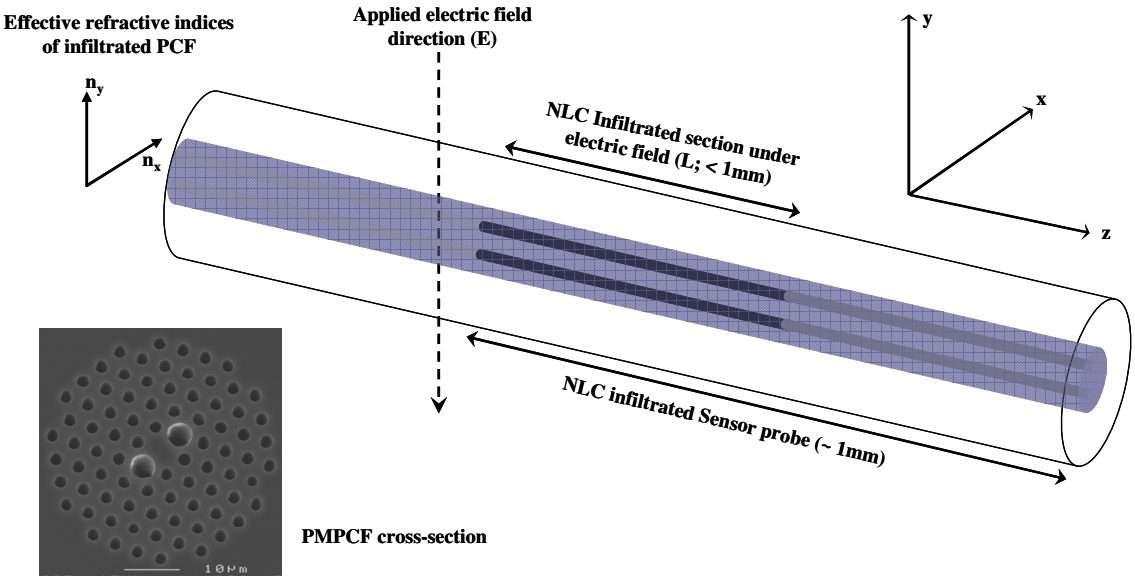
Effective refractive indices of infiltrated PCF
n_y
n_x
Applied electric field direction (E)
NLC Infiltrated section under electric field (L; < 1mm)
NLC infiltrated Sensor probe (~ 1mm)
y
x
z
PMPCF cross-section

Figure 2:

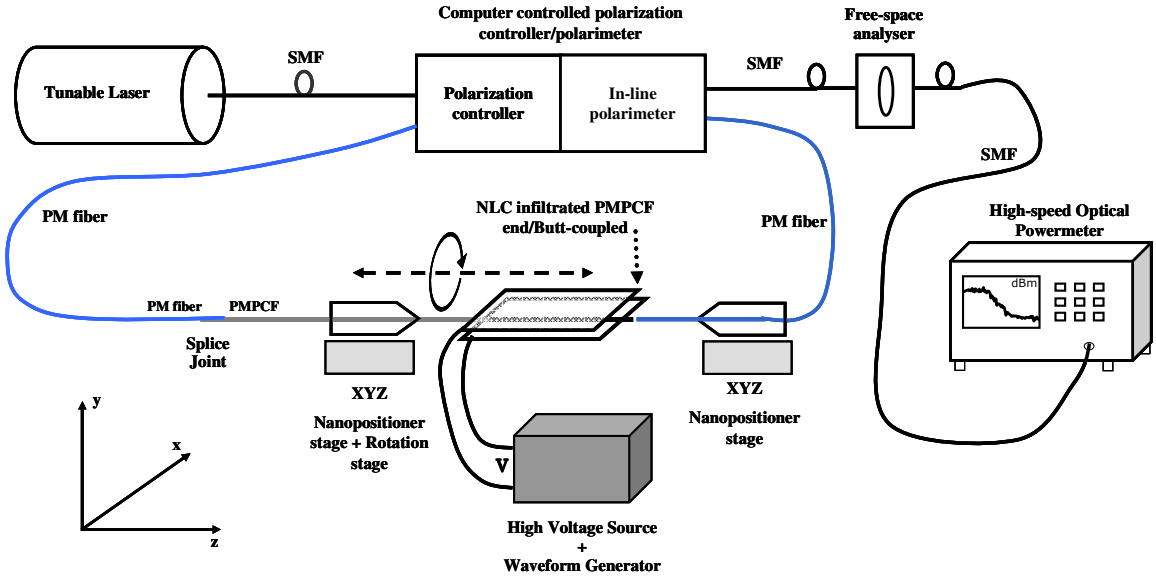
Computer controlled polarization controller/polarimeter
Free-space analyser
Tunable Laser
SMF
Polarization controller
In-line polarimeter
SMF
SMF
PM fiber
NLC infiltrated PMPCF end/Butt-coupled
PM fiber
High-speed Optical Powermeter
dBm
PM fiber
PMPCF
Splice Joint
XYZ
Nanopositioner stage + Rotation stage
XYZ
Nanopositioner stage
V
High Voltage Source + Waveform Generator
y
x
z

Figure 3:

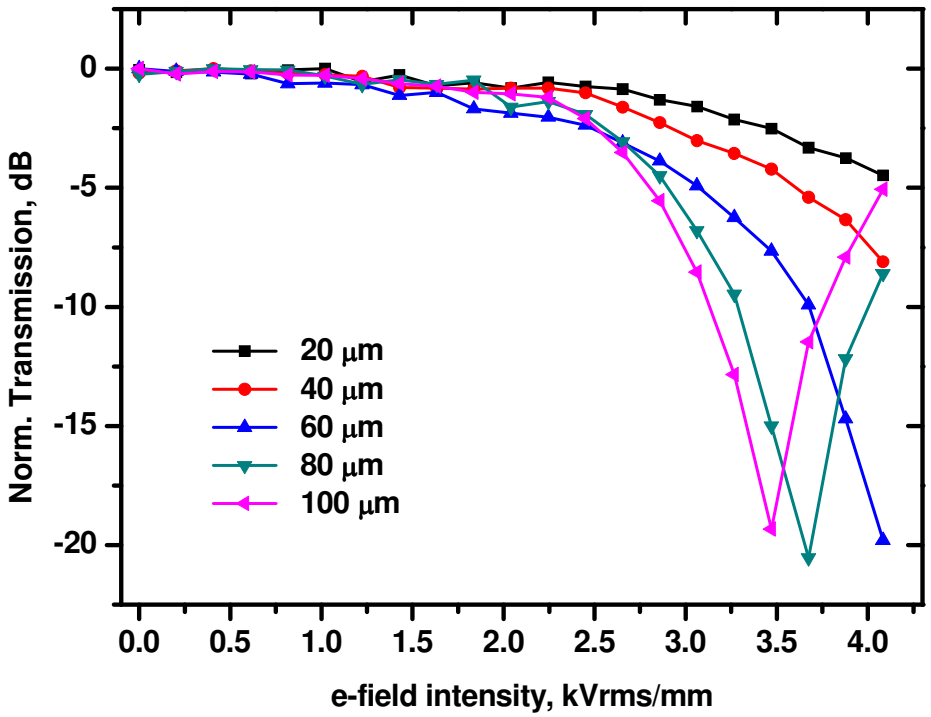
Norm. Transmission, dB
0
-5
-10
-15
-20
0.0
0.5
1.0
1.5
2.0
2.5
3.0
3.5
4.0
e-field intensity, kVrms/mm
20 μm
40 μm
60 μm
80 μm
100 μm

Figure 4:

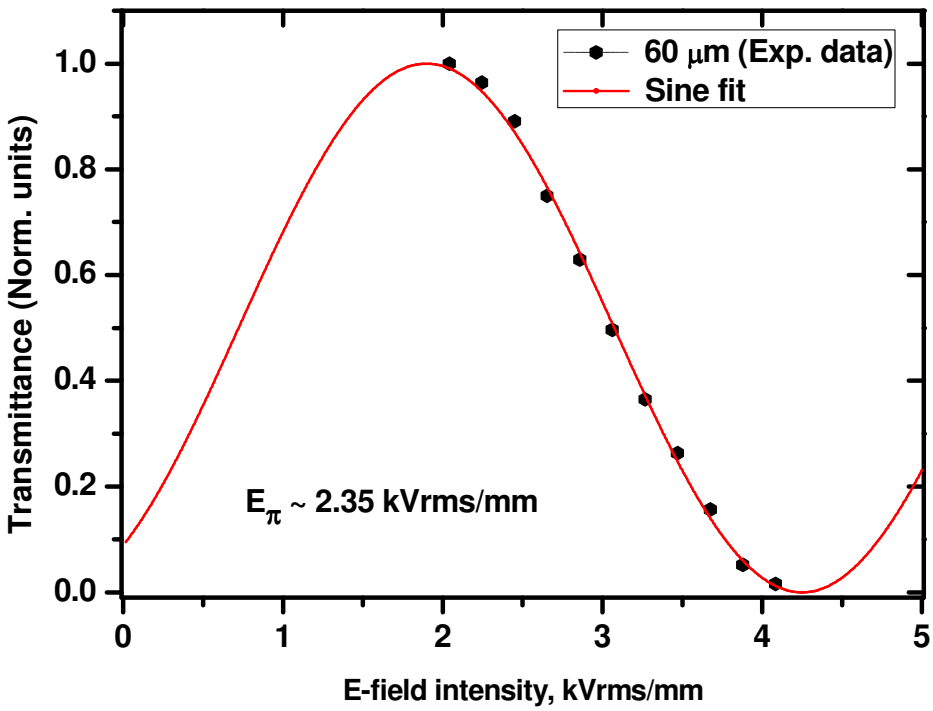
60 μm (Exp. data)
Sine fit
Transmittance (Norm. units)
E-field intensity, kVrms/mm
E_π ~ 2.35 kVrms/mm
0.0
0.2
0.4
0.6
0.8
1.0
0
1
2
3
4
5

Figure 5:

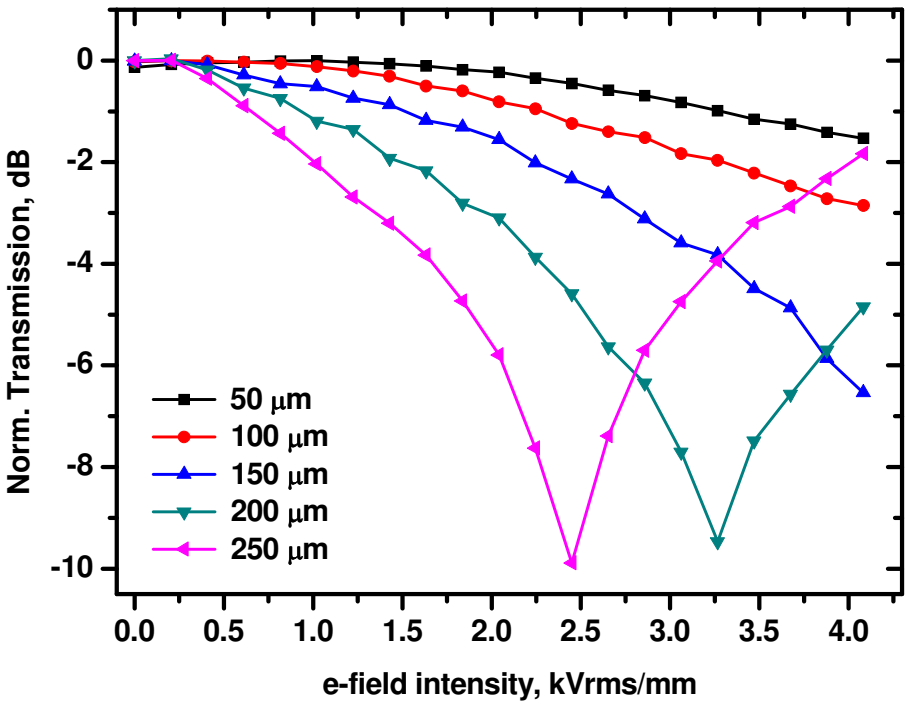
Norm. Transmission, dB
0
-2
-4
-6
-8
-10
0.0
0.5
1.0
1.5
2.0
2.5
3.0
3.5
4.0
e-field intensity, kVrms/mm
50 μm
100 μm
150 μm
200 μm
250 μm

Figure 6:

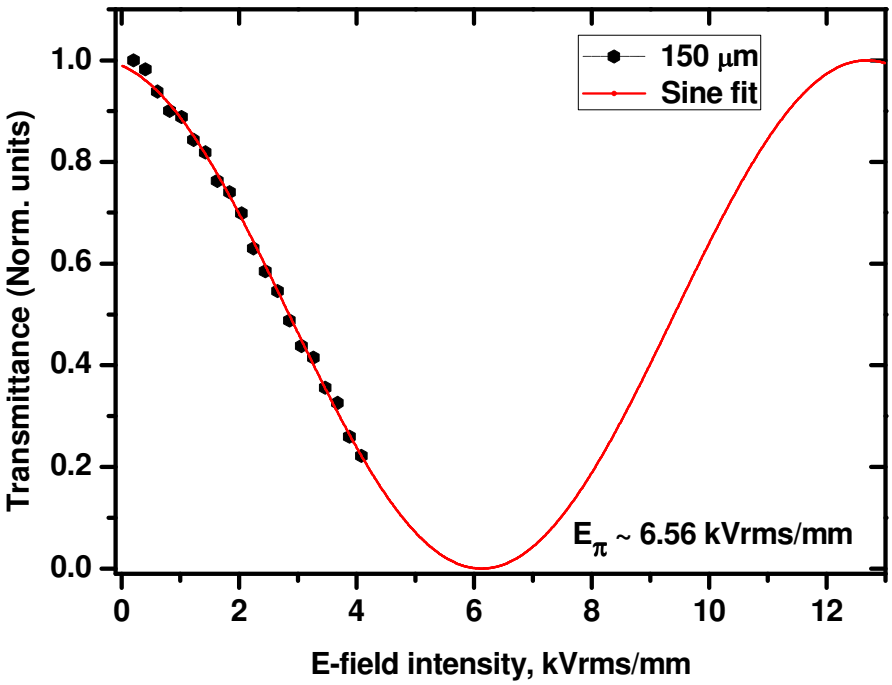
150 μm
Sine fit
E_π ~ 6.56 kVrms/mm
Transmittance (Norm. units)
E-field intensity, kVrms/mm
0.0
0.2
0.4
0.6
0.8
1.0
0
2
4
6
8
10
12